

# Mesoscopic to universal crossover of transmission phase of multi-level quantum dots

C. Karrasch,<sup>1</sup> T. Hecht,<sup>2</sup> Y. Oreg,<sup>3</sup> J. von Delft,<sup>2</sup> and V. Meden<sup>1</sup>

<sup>1</sup>*Institut für Theoretische Physik, Universität Göttingen, 37077 Göttingen, Germany*

<sup>2</sup>*Physics Department, Arnold Sommerfeld Center for Theoretical Physics, and Center for NanoScience, Ludwig-Maximilians-Universität, 80333 Munich, Germany*

<sup>3</sup>*Department of Condensed Matter Physics, The Weizmann Institute of Science, Rehovot 76100, Israel*

(Dated: September 8, 2006)

Transmission phase  $\alpha$  measurements of many-electron quantum dots (small mean level spacing  $\delta$ ) revealed universal phase lapses by  $\pi$  between consecutive resonances. In contrast, for dots with only a few electrons (large  $\delta$ ), the appearance or not of a phase lapse depends on the dot parameters. We show that a model of a multi-level quantum dot with local Coulomb correlations and arbitrary level-lead couplings reproduces the generic features of the observed behavior. The universal behavior of  $\alpha$  at small  $\delta$  follows from Fano-type antiresonances of pairs of renormalized single-particle levels.

PACS numbers: 73.23.-b, 73.63.Kv, 73.23.Hk

One of the longest-standing puzzles in mesoscopic physics is the intriguing phase-lapse behavior observed in a series of experiments [1, 2, 3] on Aharonov-Bohm rings containing a quantum dot in one arm. Under suitable conditions in linear response, both the phase and magnitude of the transmission amplitude  $T = |T|e^{i\alpha}$  of the dot can be extracted from the Aharonov-Bohm oscillations of the current through the ring. When this is done as function of a plunger gate voltage  $V_g$  that linearly shifts the dot's single-particle energy levels downward,  $\varepsilon_j = \varepsilon_j^0 - V_g$  ( $j = 1, 2, \dots$  is a level index), a series of well-separated transmission resonances [peaks in  $|T(V_g)|$ ], to be called “Coulomb blockade” (CB) peaks of rather similar width and height were observed, across which  $\alpha(V_g)$  continuously increased by  $\pi$ , as expected for Breit-Wigner-like resonances. In each CB valley between any two successive CB peaks,  $\alpha$  always jumped sharply downward by  $\pi$  (“phase lapse”, PL). The PL behavior was observed to be “universal”, occurring in a large succession of valleys for every many-electron dot studied in [1, 2, 3]. This universality is puzzling, since naively the behavior of  $\alpha(V_g)$  is expected to be “mesoscopic”, *i.e.* to show a PL in some CB valleys and none in others, depending on the dot's shape, the parity of its orbital wavefunctions, etc. Despite a large amount of theoretical work (reviewed in [4, 5]), no fully satisfactory framework for understanding the universality of the PL behavior has been found yet.

A hint at the resolution of this puzzle is provided by the most recent experiment [3], which also probed the few-electron regime: as  $V_g$  was increased to successively fill up the dot with electrons, starting from electron number  $N_e = 0$ ,  $\alpha(V_g)$  was observed to behave mesoscopically in the *few*-electron regime, whereas the above-mentioned universal PL behavior emerged only in the *many*-electron regime ( $N_e \gtrsim 15$ ). Now, one generic difference between few- and many-electron dots is that the latter have smaller level spacings  $\delta_j = \varepsilon_{j+1}^0 - \varepsilon_j^0$  for the topmost filled levels. With increasing  $N_e$ , their  $\delta_j$ 's should eventually become smaller than the respective level widths

$\Gamma_j$  stemming from hybridization with the leads. Thus, Ref. 3 suggested that a key element for understanding the universal PL behavior might be that *several overlapping single-particle levels simultaneously* contribute to transport. Due to the dot's Coulomb charging energy  $U$ , the transmission peaks remain well separated nevertheless.

Various previous works have studied the transmission amplitude of multi-level, interacting dots [6, 7, 8, 9, 10, 11, 12], including a model in which one level was assumed to be much wider than all others [8]. However, no systematic study has yet been performed of the interplay of level spacing, level widths, and charging energy that combines a wide range of parameter choices with an accurate treatment of the correlation effects induced by the Coulomb interaction. The present Letter aims to fill this gap by using two powerful methods, the numerical (NRG) [13] and functional (fRG; see [14] and references therein) renormalization group approaches, to study systems with up to 4 levels (for spinless electrons, following [12]; an analysis including spin will be published separately). We find that when the average level spacing  $\delta$  is decreased relative to the average level width  $\Gamma$ , the PL behavior of  $\alpha(V_g)$  indeed generically changes from mesoscopic (for  $\delta \gtrsim \Gamma$ ) to universal (for  $\delta \lesssim \Gamma$  and  $U \gtrsim \Gamma$ ), as observed experimentally. The universal PLs follow from Fano-type antiresonances of pairs of renormalized single-particle levels.

*Model:* The dot part of our model Hamiltonian is

$$H_{\text{dot}} = \sum_{j=1}^N \varepsilon_j n_j + \frac{1}{2} U \sum_{j \neq j'} (n_j - \frac{1}{2}) (n_{j'} - \frac{1}{2}),$$

with  $n_j = d_j^\dagger d_j$  and dot creation operators  $d_j^\dagger$  for spinless electrons, where  $U > 0$  describes Coulomb repulsion. The semi-infinite leads are described by a tight-binding model  $H_l = -t \sum_{m=0}^{\infty} (c_{m,l}^\dagger c_{m+1,l} + \text{H.c.})$  and the level-lead couplings by  $H_T = -\sum_{j,l} (t_j^l c_{0,l}^\dagger d_j + \text{H.c.})$ , where  $c_{m,l}^\dagger$  denotes the creation operator on site  $m$  of

lead  $l = L, R$  and  $t_j^l$  are real level-lead hopping matrix elements. Their relative signs for successive levels,  $s_j = \text{sgn}(t_j^L t_j^R t_{j+1}^L t_{j+1}^R)$ , are sample-dependent random variables determined by the parity of the dot's orbital wave functions. The effective width of level  $j$  is given by  $\Gamma_j = \Gamma_j^L + \Gamma_j^R$ , with  $\Gamma_j^l = \pi\rho|t_j^l|^2$ , where  $\rho$  denotes the local density of states at the end of the leads, which we take to be energy independent (wide band limit). For the chemical potential we chose  $\mu = 0$ . Our choices of  $t_j^l$  are specified below using the notation  $\sigma = \{s_1, s_2, \dots\}$ ,  $\gamma = \{\Gamma_1^L, \Gamma_1^R, \Gamma_2^L, \dots\}$ ,  $\Gamma = \frac{1}{N} \sum_{j,l} \Gamma_j^l$ .

*Methods:* We focus on linear response transport in the zero temperature limit. Then the dot produces purely elastic, potential scattering between left and right leads, characterized by the transmission matrix  $T_{ll'} = 2\pi\rho \sum_{ij} t_i^l \mathcal{G}_{ij}^R(0) t_j^{l'}$ , where  $\mathcal{G}_{ij}^R(\omega)$  is the retarded local Green function. The transmission amplitude  $T = T_{LR}$  can be expressed [15] as  $T = \sin(2\theta) \sin(\phi_a - \phi_b) e^{i(\phi_a + \phi_b)}$ , where  $e^{i2\phi_\nu}$  ( $\nu = a, b$ ) are the eigenvalues of the  $S$ -matrix  $S_{ll'} = \delta_{ll'} + iT_{ll'}$ , and the transformation  $\begin{pmatrix} \cos\theta & \sin\theta \\ -\sin\theta & \cos\theta \end{pmatrix}$  (chosen real, by time-reversal symmetry) maps the LR-basis of lead operators onto the “ab-eigenbasis” of  $S$ . Transmission zeros (TZs) and PLs occur if either  $\phi_a(V_g) - \phi_b(V_g)$  or  $\theta(V_g)$  go through zero. For LR symmetry,  $\Gamma_i^L = \Gamma_i^R$ , we have  $\theta = \pi/4$  and each level couples to only one of the leads  $a$  or  $b$ . The Friedel sum rule  $\phi_\nu = \pi\phi_\nu$  then relates  $\phi_\nu$  to the total occupancies  $n_\nu$  of all levels coupled to effective lead  $\nu$ , which we calculate by NRG. A PL occurs whenever  $n_a = n_b \bmod 1$  [Figs. 1(b,e,h), 2(c,f): black dashed, dashed-dotted lines]. The likelihood for this to happen between two CB resonances increases as  $\delta/\Gamma$  decreases, since overlapping levels of unequal widths tend to undergo occupation inversions [8, 9, 10, 11], where the wider level is filled up partially first, then is emptied by Coulomb repulsion when the narrower one fills up, causing their occupancies to cross.

In the absence of LR-symmetry, knowledge of  $\phi_\nu(V_g)$  is insufficient to determine  $T(V_g)$ , since  $\theta$  becomes  $V_g$ -dependent too. E.g.,  $\theta(V_g)$  passes through zero when the  $V_g$ -dependent level-lead coupling for one of the levels changes from being stronger for lead  $a$  to being stronger for lead  $b$ . For general couplings, we thus obtain  $T$  directly by using fRG to calculate  $\mathcal{G}_{ij}^R$ . The fRG is a renormalization scheme for the self-energy  $\Sigma$  and higher order vertex functions (see [14] for details). We use a truncation scheme that keeps only the flow equations for  $\Sigma$  and for the frequency independent part of the effective two-particle (Coulomb) interaction. Comparisons with NRG [14] have shown this approximation to be reliable provided that the number of (almost) degenerate levels and the interaction do not become too large. fRG is also much cheaper computationally than NRG, enabling us to explore efficiently the vast parameter space relevant for multi-level dot models; e.g. we computed roughly  $5 \times 10^7$  data points to obtain a comprehensive picture for  $N = 3$ . At the end of the fRG flow, the full Green function at

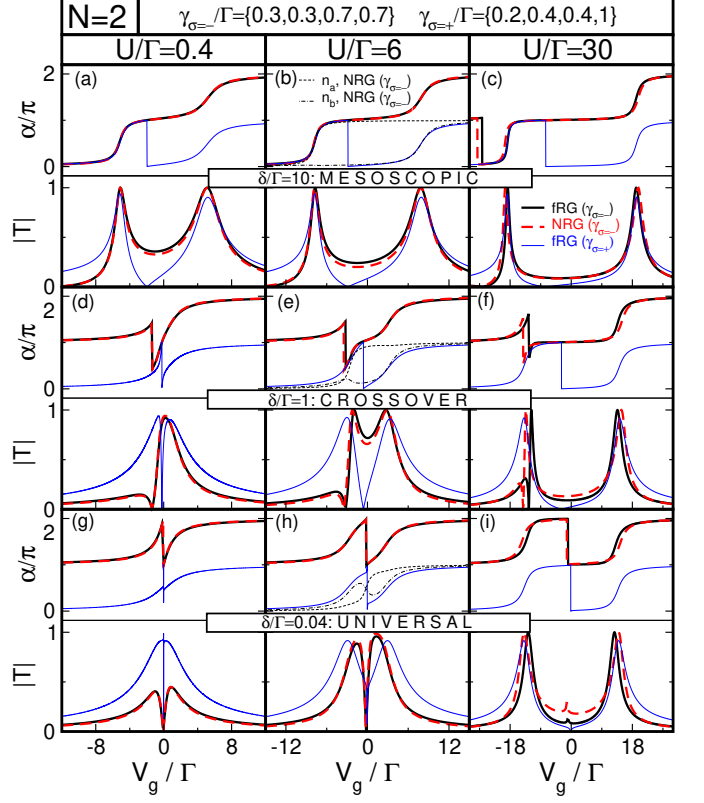


FIG. 1:  $|T(V_g)|$  and  $\alpha(V_g)$  for  $N = 2$  and  $\varepsilon_{2,1}^0 = \pm\delta/2$ : decreasing  $\delta/\Gamma$  produces a change from (a,b,c) mesoscopic via (d,e,f) crossover to (g,h,i) universal behavior; increasing  $U/\Gamma$  produces increased transmission peak spacing. (b,e,h) include the occupancies  $n_a$  (thin dashed) and  $n_b$  (thin dash-dotted) of the narrower or broader level in the case of LR-symmetry, illustrating that occupation inversion produces a TZ and PL. (i) For  $\delta/\Gamma < 1$  and sufficiently large  $U$ , the CB peaks lie at  $V_g \approx \pm U/2$ . They have equal height and equal full width significantly larger than  $\Gamma$  [not  $2\Gamma_j$ , as in (c)], showing that both bare single-particle levels simultaneously contribute to transport. For the blip and hidden TZ near  $V_g = 0$ , see [16].

zero frequency takes the form  $[\mathcal{G}^R(0)]_{ij}^{-1} = -h_{ij} + i\Delta_{ij}$ , with  $\Delta_{ij} = \pi\rho \sum_l t_i^l t_j^l$  and an effective, *noninteracting* (but  $V_g$  and  $U$ -dependent) single-particle Hamiltonian  $h_{ij} = (\varepsilon_j^0 - V_g)\delta_{ij} + \Sigma_{ij}$ . To interpret our results, it is useful to adopt the eigenbasis of  $[\mathcal{G}^R(0)]_{ij}^{-1}$ , the eigenvalues of which we denote  $-\tilde{\varepsilon}_j + i\tilde{\Gamma}_j$ , to arrive at a renormalized effective model (REM). Our fRG approach describes how interference of transmissions through all the bare levels of the dot in the presence of interactions lead to renormalized level positions  $\tilde{\varepsilon}_j$  and widths  $\tilde{\Gamma}_j$ .

*Results:* Our results are illustrated in Figs. 1 to 3. fRG and NRG data generally coincide rather well (compare black and red lines in Figs. 1 and 2), except for  $N = 4$  when both  $U \gg \Gamma$  and  $\delta \ll \Gamma$ , in which case correlations become very strong and fRG unreliable [14]. The figures illustrate the following striking qualitative features, that we have found to be generic, *i.e.* typical for an overwhelming part of parameter space (the importance of going beyond symmetric choices of level-lead

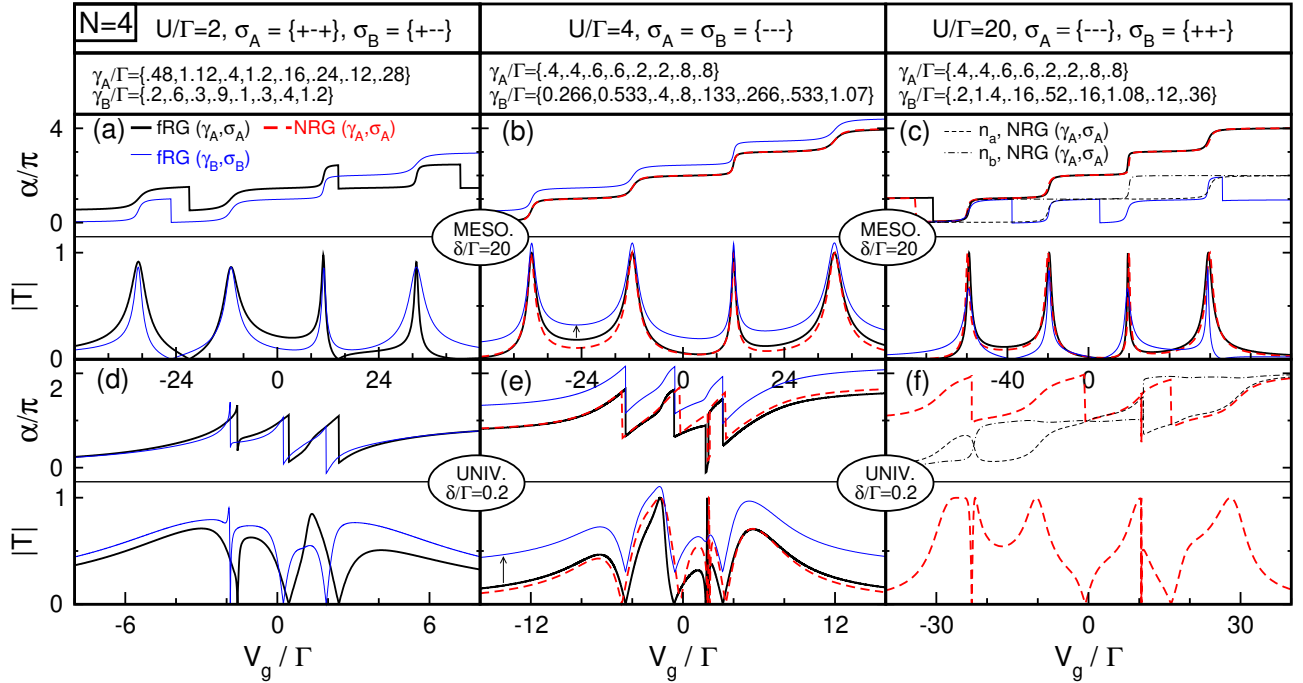


FIG. 2:  $|T(V_g)|$  and  $\alpha(V_g)$  for  $N = 4$ , with all level spacings taken to be equal,  $\delta_j \equiv \delta$ . The qualitative features do not change if this assumption is relaxed, or if  $U$  is assumed to be slightly level-dependent,  $U \rightarrow U_{jj'}$ . Decreasing  $\delta/\Gamma$  produces a crossover from (a,b,c) mesoscopic to (d,e,f) universal behavior; increasing  $U/\Gamma$  produces increased transmission peak spacing. (e) shows that double Tzs and PLs disappear with increasing asymmetry. In (b,e), the “B”-curves were shifted upwards, for clarity, by the length of the arrow. (f) illustrates universal behavior for the phase as experimentally observed.

couplings was emphasized in [11, 12] for  $N = 2$ ):

*Mesoscopic regime:* For  $\delta \gtrsim \Gamma$  [Figs. 1(a,b,c), 2(a,b,c), 3(c)], we recover behavior that is similar to the  $U = 0$  case. Within the REM it can be understood as transport occurring through only one effective level at a time [see Fig. 3(a,b,c)]. Each  $\tilde{\varepsilon}_j$  that crosses the chemical potential gets filled by an electron and a Breit-Wigner-like transmission resonance occurs at  $\tilde{\varepsilon}_j \approx 0$ . The renormalized energies pick up a shift ( $j - \frac{1}{2}[N + 1]U$ ) across the  $j$ ’th CB peak, while the  $\tilde{\Gamma}_j$  are hardly renormalized ( $\simeq \Gamma_j$ ). As in the noninteracting case the full width of the CB peaks is thus  $2\Gamma_j$  and its height governed by the asymmetry of  $\Gamma_j^{L/R}$ . The peak separation is given by the level spacing  $\delta_j + U$ . Between two peaks,  $\alpha(V_g)$  behaves mesoscopically: depending on the sign  $s_j$  one either observes a PL ( $s_j = +$ ) or continuous evolution of  $\alpha$  ( $s_j = -$ ) [17, 18]. Additional PLs occur far left or right, beyond the last transmission peak [12].

*Mesoscopic to universal crossover:* As the ratio  $\delta/\Gamma$  is reduced, the behavior changes dramatically: the Tzs and PLs that used to be on the far outside move inward across CB resonances [see evolution in Figs. 1(b,e,h)].

*Universal regime:* A universal feature emerges for sufficiently small  $\delta/\Gamma$  and sufficiently large  $U/\Gamma$  (the crossover scales for both are order 1, but depend rather strongly on the chosen parameters  $\gamma$ ,  $\sigma$ , and  $N$  [19]): for all choices of the signs  $\sigma$  and generic couplings  $\gamma$ , the  $N$  CB peaks over which  $\alpha$  increases by  $\pi$  are separated by  $N - 1$  PLs, each accompanied by a TZ [Figs. 1(g,h,i), 2(d,e,f), 3(f)]. This is qualitatively consistent with the experimentally

observed trend. For small to intermediate values of  $U/\Gamma$  [Figs. 1(g,h), 2(d,e)], the transmission peaks are not well-separated, and  $\alpha(V_g)$  has a saw-tooth shape. As  $U/\Gamma$  increases, the transmission peaks become better separated and the corresponding phase rises take a more S-like form [Figs. 1(h,i), 2(e,f)]. For  $U/\Gamma$  as large as in Figs. 1(i) and 2(f), the behavior of  $\alpha(V_g)$  (both the S-like rises and the universal occurrence of PLs in each valley) is very reminiscent of that observed experimentally.

For certain fine-tuned parameter sets ( $\gamma$  and  $\sigma$ ) the behavior at small  $\delta/\Gamma$  deviates from the generic case discussed above. For  $N = 2$  the non-generic cases were classified in [11]. For  $N = 3, 4$  and *LR-symmetry* [Fig. 2(e,f)], curves “A” we find that an additional feature appears:  $|T|$  and  $\alpha$  can have a closely-spaced “double zero” and “double phase jump” (by  $\mp\pi$ ), respectively. However, these sharp features are presumably irrelevant to the experiments as they quickly disappear upon switching on LR-asymmetry, as shown in Fig. 2(e) (blue line). In any case they are so sharp that they would be hard to resolve.

*Interpretation:* We can gain deeper insight into the appearance of the Tzs and PLs in the universal regime from the properties of the REM obtained by fRG. Fig. 3(d,f) shows an example of the generic  $V_g$ -dependence of  $\tilde{\varepsilon}_j$  and  $\tilde{\Gamma}_j$  for  $N = 3$ , together with  $|T|$  and  $\alpha$ . For all parameter sets with  $\delta < \Gamma$  studied, sufficiently large interactions (i) amplify (generic) asymmetries in the bare  $\Gamma_j$  leading to a single wide level [20] and  $N - 1$  significantly narrower levels [21], and (ii) lead to  $\tilde{\varepsilon}_j$  which depend nonmonotonically on  $V_g$  [in contrast for  $\delta \gtrsim \Gamma$  the trends (i) and

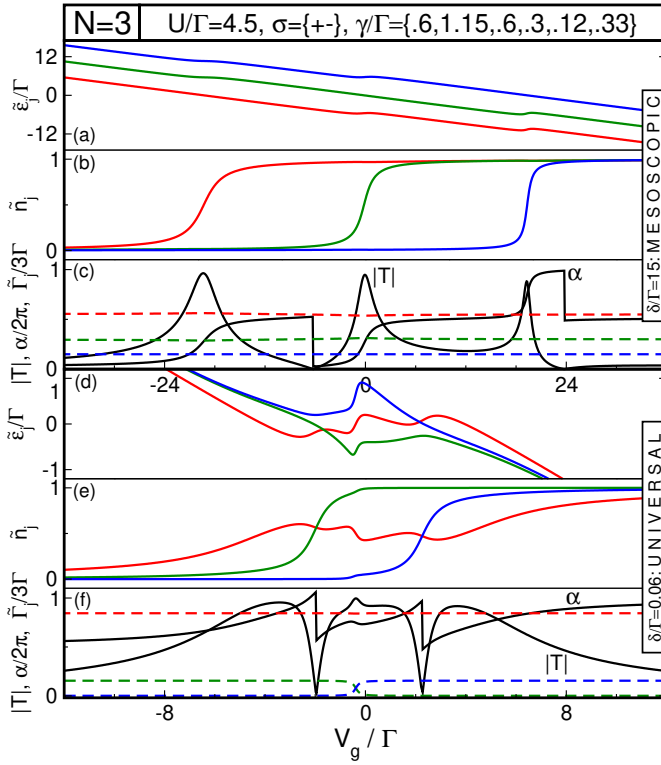


FIG. 3: Renormalized single-particle energies  $\tilde{\varepsilon}_j$ , occupancies  $\tilde{n}_j$  and level widths  $\tilde{\Gamma}_j$  (dashed) of the REM, and the resulting  $|T|$  and  $\alpha$  (all as functions of  $V_g$ ), for  $N = 3$  and  $\delta_j \equiv \delta$ .

(ii) are very much weaker; Fig. 3(a,c)]. Close to the TZs and PLs the wide level is close to zero *and* one of the narrow levels [crossings in Fig. 3(d)]. This leads to a Fano-type effect [22, 23, 24] and each TZ, and thus PL, can be understood as a Fano antiresonance arising from destructive interference between two transmission paths through the dot. Note that the occurrence of destructive interference is independent of the relative signs of the level-lead couplings. Since each TZ is accompanied by an occupation inversion of the effective levels [Fig. 3(e)], this explanation can be viewed as a generalization of our earlier observation for LR-symmetry.

*Conclusions:* The most striking feature of our results, based on exhaustive scans through parameter space for  $N = 2, 3, 4$ , is that for any given, generic choice of couplings ( $\gamma$  and  $\sigma$ ), the experimentally observed crossover [3] from mesoscopic to universal  $\alpha(V_g)$ -behavior can be achieved within our model by simply changing the ratio  $\delta/\Gamma$  from  $\gtrsim 1$  to  $\lesssim 1$ , provided that  $U/\Gamma \gtrsim 1$ . Within a renormalized effective single-particle picture, at each PL in the universal regime electrons passing through a broad and a narrow level interfere destructively, producing a Fano-type antiresonance. This appears to be at the heart of the universal phase lapse behavior [1, 2, 3]. A quantitative description requires correlations to be treated accurately. We expect that the main features of this mechanism will carry over to the case of spinful electrons and finite temperatures – showing this explicitly would be an interesting challenge for future work.

We thank P. Brouwer, Y. Gefen, L. Glazman, D. Golosov, M. Heiblum, J. Imry, J. König, F. Marquardt, M. Pustilnik, H. Schoeller, K. Schönhammer, and A. Silva for valuable discussions. This work was supported in part by the DFG, for VM by SFB602; for TH and JvD by SFB631, Spintronics RTN (HPRN-CT-2002-00302), NSF (PHY99-07949) and DIP-H.2.1; and for YO by DIP-H.2.1, BSF and the Humboldt foundation.

- [1] Y. Yacoby *et al.*, Phys. Rev. Lett. **74**, 4047 (1995).
- [2] R. Schuster *et al.*, Nature **385**, 417 (1997).
- [3] M. Avinun-Khalish *et al.*, Nature **436**, 529 (2005).
- [4] G. Hackenbroich, Phys. Rep. **343**, 463 (2001).
- [5] Y. Gefen in *Quantum Interferometry with Electrons: Outstanding Challenges*, I. V. Lerner *et al.*, eds. (Kluwer, Dordrecht, 2002), p. 13.
- [6] C. Bruder, R. Fazio, and H. Schoeller, Phys. Rev. Lett. **76**, 114 (1995).
- [7] Y. Oreg and Y. Gefen, Phys. Rev. B **55**, 13726 (1997).
- [8] P.G. Silvestrov and Y. Imry, Phys. Rev. Lett. **85**, 2565 (2000); Phys. Rev. B **65**, 035309 (2001).
- [9] J. König and Y. Gefen, Phys. Rev. B **71**, 201308(R) (2005).
- [10] M. Sindel, A. Silva, Y. Oreg, and J. von Delft, Phys. Rev. B **72**, 125316 (2005).
- [11] V. Meden and F. Marquardt, Phys. Rev. Lett. **96**, 146801 (2006).
- [12] D.I. Golosov and Y. Gefen, cond-mat/0601342.
- [13] H. R. Krishna-murthy, J. W. Wilkins, and K. G. Wilson, Phys. Rev. B **21**, 1003 (1980).
- [14] C. Karrasch, T. Enss, and V. Meden, Phys. Rev. B **73**, 235337 (2006).
- [15] M. Pustilnik and L. I. Glazman, Phys. Rev. Lett. **87**, 216601 (2001).
- [16] For  $N = 2$ ,  $U$  larger than a critical value and in the limit  $\delta \rightarrow 0$ , two additional, very sharp peaks appear on both sides of and exponentially close to the TZ near  $V_g = 0$  (peaks and TZ are visible only as a blip in Fig. 1(i), due to lack of resolution) [11]. Similar sharp features occur for  $N > 2$ , see Fig. 2(f). We believe that these features, which presumably will get smeared out with increasing temperature, are irrelevant for the PL puzzle.
- [17] A. Silva, Y. Oreg, and Y. Gefen, Phys. Rev. B **66**, 195316 (2002).
- [18] T.-S. Kim and S. Hershfield, Phys. Rev. B **67**, 235330 (2003).
- [19] For  $\delta \lesssim \Gamma$ , generic  $\Gamma_j^l$  and  $N = 2$ , the universal PL behavior (1 PL between the two CB peaks) already occurs at  $U = 0$ . For  $N > 2$  and small  $U/\Gamma$ , universal behavior ( $N - 1$  PL between  $N$  CB peaks) sets in only once  $U/\Gamma$  becomes large enough [as is already the case in Fig. 2(d)].
- [20] We emphasize that for  $\delta \lesssim \Gamma$  and  $U \gtrsim \Gamma$  a renormalized wide level is generated for *generic* couplings, in contrast to Ref. 8, which introduces a wide bare level as a model assumption (as does [22]). Also, whereas in [8] the wide level repeatedly empties into narrow ones as  $V_g$  is swept, this does not always occur in our scenario, see Fig. 3(e).
- [21] We find that for those *narrow* levels that contribute to transport, with  $|\tilde{\varepsilon}_j(V_g)| \lesssim \tilde{\Gamma}_j(V_g)$ , the Thouless criterion  $\tilde{\Gamma} \lesssim \tilde{\delta}$  holds, and that Coulomb blockade physics survives.
- [22] Y. Oreg, in preparation.

- [23] U. Fano, Phys. Rev. **124**, 1866 (1961).
- [24] A.A. Clerk, X. Waintal, and P.W. Brouwer, Phys. Rev. Lett. **86**, 4639 (2001).